Experimental Demonstration of Electromagnetic Tunneling Through an Epsilon-Near-Zero Metamaterial at Microwave Frequencies

Ruopeng Liu
Department of Electrical and Computer Engineering, Duke University, Durham, North Carolina 27708, USA

Qiang Cheng
State Key Laboratory of Millimeter Waves, Southeast University, Nanjing 210096, China

Thomas Hand and Jack J. Mock
Department of Electrical and Computer Engineering, Duke University, Durham, North Carolina 27708, USA

Tie Jun Cui*
State Key Laboratory of Millimeter Waves, Southeast University, Nanjing 210096, China

Steven A. Cummer and David R. Smith†
Center for Metamaterials and Integrated Plasmonics, Department of Electrical and Computer Engineering, Duke University, Durham, North Carolina 27708, USA

(Received 23 March 2007; revised manuscript received 4 November 2007; published 18 January 2008)

Silveirinha and Engheta have recently proposed that electromagnetic waves can tunnel through a material with an electric permittivity (ϵ) near zero (ENZ). An ENZ material of arbitrary geometry can thus serve as a perfect coupler between incoming and outgoing waveguides with identical cross-sectional area, so long as one dimension of the ENZ is electrically small. In this Letter we present an experimental demonstration of microwave tunneling between two planar waveguides separated by a thin ENZ channel. The ENZ channel consists of a planar waveguide in which complementary split ring resonators are patterned on the lower surface. A tunneling passband is found in transmission measurements, while a two-dimensional spatial map of the electric field distribution reveals a uniform phase variation across the channel—both measurements in agreement with theory and numerical simulations.

DOI: 10.1103/PhysRevLett.100.023903 PACS numbers: 41.20.Jb, 42.25.Bs, 78.20.Ci, 84.40.Az

The available palette of electromagnetic properties has expanded considerably over the past several years due to the development of artificially structured materials, or metamaterials. In particular, metamaterials whose relative constitutive parameters—such as the electric permittivity ϵ or the magnetic permeability μ—are less than unity have proven to exhibit a remarkable influence on wave propagation properties, and have thus become a vigorous research topic [1–3].

Much attention has recently focused on structures for which the real part of one or both of the constitutive parameters approaches zero. These structures have been used to form interesting devices such as highly directive antennas [4] and compact resonators [5]. Most recently, Silveirinha and Engheta [6] have proposed that a material whose electric permittivity is near zero—or an epsilon-near-zero (ENZ) medium—can form the basis for a perfect coupler, coupling guided electromagnetic waves through a channel with arbitrary cross section. While it might at first be thought that the inherent impedance mismatch between an ENZ medium and any other medium should degrade the transmission efficiency, remarkably this turns out not to be the case so long as at least one of the physical dimensions of the ENZ material channel is electrically small.

In this Letter, we make use of planar complementary split ring resonators (CSRRs) patterned in one of the ground planes of a planar waveguide to form the electromagnetic equivalent of an ENZ. The CSRR structure was proposed by Falcone *et al.* [7], who showed by use of the Babinet principle that the CSRR has an electric resonance that couples to an external electric field directed along the normal of the CSRR surface. It was further shown explicitly that a volume bounded by a CSRR surface behaves identically to a volume containing a resonantly dispersive dielectric. Variants of the wire medium could also potentially be used to form the ENZ medium [8], though spatial dispersion and effects due to the finite wire length can cause significant complication [9].

The geometry considered here to demonstrate the tunneling effect is chosen to be compatible with our planar waveguide experimental apparatus (Fig. 1) previously described [10]. Three distinct waveguide sections are formed, distinguished by the differing gap heights between the upper and lower metal planes. There is a gap of 11 mm between the upper and lower conducting plates that serve as the input and output waveguides. The narrowed tunneling channel with patterned CSRRs in the lower surface has a gap of 1 mm between the plates. The planar waveguide is

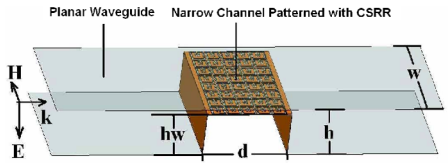

FIG. 1 (color online). Experimental setup, in which $h = 11$ mm, $hw = 10$ mm, $d = 18.6$ mm (16.6 mm for CSRR regime), and $w = 200$ mm. Lower figure is the sample inside chamber.

bounded on either side by layers of absorbing material, which approximate magnetic boundary conditions and also reduce reflection at the periphery. The waveguide and channel thus support waves that are nearly transverse electromagnetic (TEM) in character. Assuming the CSRR region can be treated as a homogenized medium, the entire configuration is well approximated as two dimensional, with the average field distribution having little variation along the width.

There are three impedances that can be defined for the waveguide geometry used here [11]: the intrinsic, wave, and characteristic impedances. The wave impedances corresponding to TEM waves in the three waveguide regions are equivalent irrespective of the waveguide shape, all equal to Z_1. However, the characteristic impedance is defined by the equivalent voltage and equivalent current of the transmission line [11], which are dependent on the cross sections of the waveguides. There is thus a severe characteristic impedance mismatch at the two interfaces between the planar waveguides and the narrow channel that inhibits the transmission of waves from the left waveguide region to the right. A characteristic impedance model for the specific geometry considered here has been described in detail in [12], where a transmission-line model is derived showing that the narrow waveguide region can be replaced by a region having an impedance $Z_2 = (d/b)Z_1$. d/b is the ratio of the planar waveguide and channel heights. In addition, there is a shunt admittance $Y = jB$ at the interface between the mismatched waveguides, which becomes quite large (and therefore unimportant) when the waveguides differ significantly in height. Because $Z_2 \ll Z_1$, there is no coupling between the input and output waveguides, except possibly when a resonance condition is met and a Fabry-Perot oscillation occurs. If the channel is now loaded with an ENZ material, the characteristic impedance of the channel region is raised to the point where the three waveguide regions are matched and perfect transmission once again should occur.

The experimental configuration studied here corresponds to one of the two cases considered by Silveirinha and Engheta [6]. In the first case ϵ and μ tend to zero simultaneously, while in the second ϵ is near zero and the area of channel is assumed electrically small. Our experimental setup belongs to the latter case, whose mechanism is illustrated by calculating the reflectance based on the simplified model described in [12]. We find

$$R = \frac{R_{12}(1 - e^{i2k_{2z}d})}{1 - R_{12}^2 e^{i2k_{2z}d}} \tag{1}$$

in which $R_{12} = (Z_2//(-iB) - Z_1)/(Z_2//(-iB) + Z_1)$ and $Z_2//(-iB) = (-iBZ_2)/(-iB + Z_2)$. R_{12} is the reflection coefficient between the planar waveguide and the channel, d is the effective length of the channel, and k_{2z} is the wave vector inside the channel. Z_1 and Z_2 are the effective wave impedances outside and inside the narrow channel, respectively, whose ratio Z_1/Z_2 corresponds to the height ratio 11/1 [12] in the absence of the patterned CSRRs. When ϵ and μ are simultaneously near zero, the characteristic impedance of the zero index material may take on the finite value $\lim_{\epsilon,\mu\to 0}\sqrt{\mu/\epsilon}$, which may differ from the impedance of adjacent regions. However, since $k \to 0$, the reflection coefficient vanishes, indicating the tunneling of the wave across the channel [6]. In the present configuration, since Z_2/Z_1 approaches zero, the reflection coefficient no longer vanishes in a simple manner. Instead, when the ENZ medium possesses a small but finite value of permittivity, Z_2/Z_1 may approach unity, and the tunneling effect is restored.

The equivalence between an ENZ metamaterial and the CSRR structure shown in Fig. 2 can be established by performing a numerical retrieval of the effective constitutive parameters for the channel. To obtain the retrieved permittivity shown in Fig. 2, the scattering (S) parameters are simulated using Ansoft HFSS, a commercial full-wave electromagnetic solver [13–16]. Figure 2(b) shows the simulation setup used to retrieve the effective constitutive parameters of the CSRR channel. The polarization of the incident TEM wave is constrained by the use of perfect magnetic conducting (PMC) boundaries on the sides of the computational domain. The separation between the metal plates in the channel region is $h = 1$ mm, while the vacuum region has a height of $d = 11$ mm with a perfect electric conducting (PEC) boundary on the lower surface. Radiation boundaries are assigned below the ports, as shown in the figure. The two ports are positioned far away from the CSRR structure to avoid near-field cross coupling between the ports and the CSRRs; however, the phase reference planes for the retrieval are chosen (or deembedded) to be just on either side of the channel.

The simulated reflection and transmission coefficients as a function of frequency for the channel with and without the ENZ metamaterial are shown in Fig. 4. These results are compared with the simplified model presented in Eq. (1), where $Z_2 = Z_1/(11\sqrt{\epsilon_{\mathrm{eff},r}})$ with the effective length d chosen as 13 mm. An approximate analytical expression for B obtained by a conformal mapping procedure is presented in [12]. The transmission and reflection coefficients predicted by the analytical model are plotted in Fig. 4, where they can be seen to be in very good agreement with those simulated, supporting the interpretation of the transmission peak as an indication of tunneling. In addition, Fig. 3(a) shows the Poynting vector distribution at

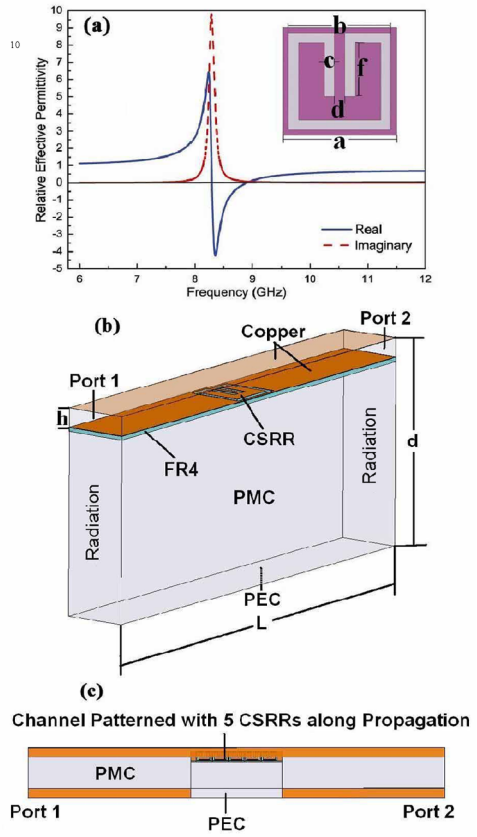

FIG. 2 (color online). Retrieval results, dimensions of CSRRs, and simulation setup. (a) Extracted permittivity and CSRRs' dimensions, in which $a = 3.333$ mm, $b = 3$ mm, $c = d = 0.3$ mm, and $f = 1.667$ mm. (b) Simulation configuration for CSRR unit cell. $d = 11$ mm, $h = 1$ mm, and $L = 23.333$ mm. (c) Configuration of tunneling effect simulation.

8.8 GHz, revealing the squeezing of the waves through the narrow channel.

To validate experimentally the ENZ properties of the CSRR region, a channel patterned with CSRRs was fabricated and its scattering compared to an unpatterned control channel. Both the CSRR and control channels were formed from copper-clad FR4 circuit board (0.2 mm thick), fabricated with dimensions 18.6×200 (mm^2) (shown in Fig. 1). The array of CSRR elements (shown in Fig. 2) was patterned on the circuit board using standard photolithography. A total of 200 CSRRs (5 in the propagation direction, 40 in the transverse direction) were used to form the effective ENZ metamaterial. The CSRR or control substrates were then placed on a Styrofoam support, with dimensions $18.6 \times 10 \times 200$ (mm^3). Copper tape was used to cover the sides of the Styrofoam and carefully placed to ensure that the copper-clad substrates would make good electrical contact with the bottom plate of the waveguide.

To obtain a base level of transmission, the control sample was positioned inside the planar waveguide halfway between the two ports and a transmission measurement taken. The results are shown in Fig. 4 and compared with

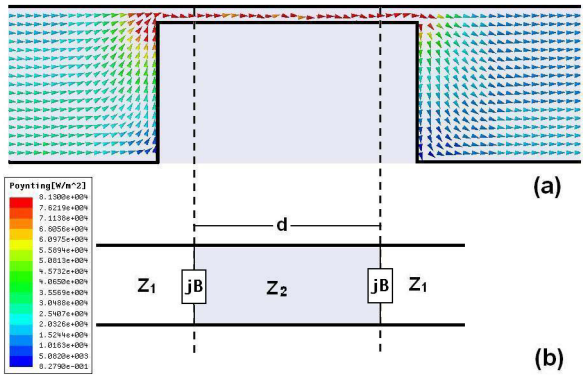

FIG. 3 (color online). Poynting vector and medium model: (a) Poynting vector. (b) Simplified model.

both the analytical model and the HFSS simulation. The passband of the control slab, due to the resonance condition, was found to occur at 7 GHz—shifted from the passband found in simulation. The consistent shift between measurement and simulation likely reflects the differences between the experimental environment and the simulation model (e.g., finite slab width and fluctuation of channel height). The measurement and simulation, however, are in excellent qualitative agreement. By uniformly shifting the frequency scale, the measured and simulated curves are almost identical (note the two scales indicated on the top and bottom axes).

With the control slab replaced by the CSRR channel, the measured transmitted power (shown in Fig. 4) reveals a passband near 7.9 GHz (8.8 GHz from the simulation), which is identical with retrieval prediction. This passband is absent when the control slab is present, demonstrating that electromagnetic tunneling takes place at approximately the frequency where the effective permittivity of the ENZ region approaches zero.

Phase sensitive maps of the spatial electric field distribution throughout the channel region were constructed [10]. The electric field magnitude was mapped inside a

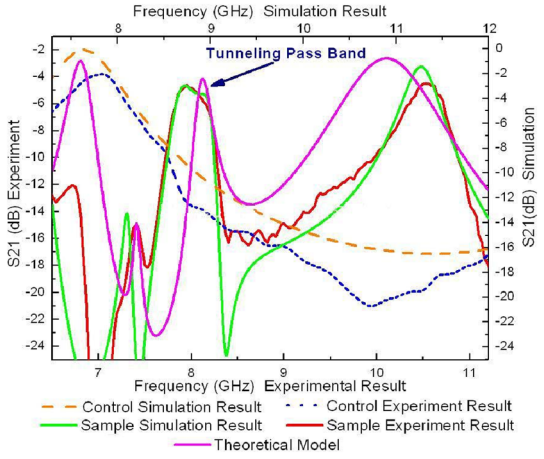

FIG. 4 (color online). Experimental, theoretical, and simulated transmissions for the tunneling and control samples.

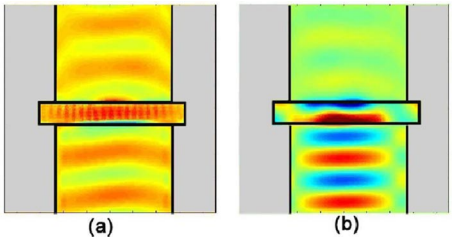

FIG. 5 (color online). Two-dimensional mapper results at 8.04 GHz. (a) Field distribution of tunneling sample. (b) Field distribution of control.

180×180 (mm^2) square region for both the copper control and CSRR channels. Figure 5 shows the mapped fields for both configurations taken at 8.04 GHz (where the effective permittivity of the CSRR structure is approximately zero). The field is normalized by the average field strength. Yet it is clear that the CSRR channel allows transmission of energy to the second port, measured to be -5 dB, whereas only -14 dB of field energy propagates to port 2 when the control slab is presented. Note the uniform phase variation across the channel at the tunneling frequency, $f = 8.04$ GHz.

A linear plot of phase versus position (shown in Fig. 6) further illustrates the tunneling of energy through the ENZ channel versus the Fabry-Perot–like resonant scattering. The latter mechanism of transmission has been studied in detail by Hibbins *et al.* [17]. As can be seen in Fig. 6, a strong phase variation exists across the control channel at $f = 7$ GHz, corresponding to the passband that is seen in Fig. 3. The clearly distinguished phase advance within the channel implies that the propagation constant is nonzero. The large transmittance results from a resonance condition related to the length of the channel. By contrast, the spatial phase variation for the CSRR channel is shown in Fig. 6 for $f = 8.04$ GHz (the passband of the CSRR loaded channel), where we see that the phase advance across the channel at this frequency is negligible.

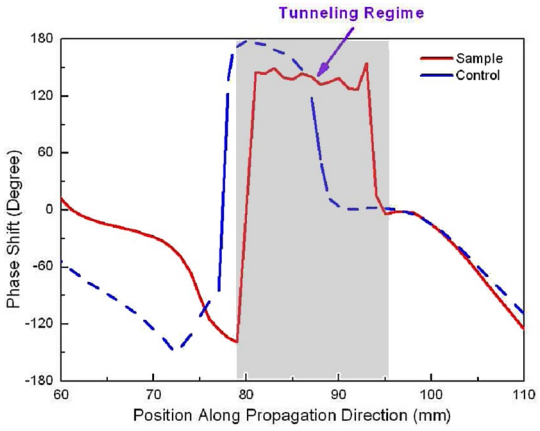

FIG. 6 (color online). Phase shift for 5 unit-cell tunneling sample at 8.04 GHz and control at 7 GHz.

While the CSRR waveguide used in these experiments does not form a volumetric metamaterial, we have nevertheless shown that the planar waveguide channel can be treated equivalently as having a well-defined resonant permittivity, with zero value at a frequency of 8.04 GHz. Furthermore, the set of transmission and mapping measurements we have presented demonstrates that the tunneling observed through the channel is consistent with the behavior of an ϵ-near-zero medium. The measurements confirm that ''squeezed waves'' will tunnel without phase shift through extremely narrow ENZ channels. ENZ materials may thus be used as highly efficient couplers with broad application in microwave and THz devices.

This work was supported by the Air Force Office of Scientific Research through a Multiple University Research Initiative, Contract No. FA9550-06-1-0279. T. J. C. acknowledges support from the National Basic Research Program (973) of China under Grant No. 2004CB719802 and the National Science Foundation of China under Grant No. 60671015.

*tjcui@seu.edu.cn
†drsmith@ee.duke.edu

[1] D. R. Smith, Willie J. Padilla, D. C. Vier, S. C. Nemat-Nasser, and S. Schultz, Phys. Rev. Lett. **84**, 4184 (2000).
[2] D. Schurig, J. J. Mock, B. J. Justice, S. A. Cummer, J. B. Pendry, A. F. Starr, and D. R. Smith, Science **314**, 977 (2006).
[3] L. D. Landau, E. M. Lifshitz, and L. P. Pitaevskii, *Electrodynamics of Continuous Media* (Butterworth-Heinemann, Oxford, England, 1984), 2nd ed., p. 287.
[4] S. Enoch *et al.*, Phys. Rev. Lett. **89**, 213902 (2002).
[5] A. Lai, C. Caloz, and T. Itoh, IEEE Microw. Mag. **5**, 34 (2004).
[6] M. Silveirinha and N. Engheta, Phys. Rev. Lett. **97**, 157403 (2006).
[7] F. Falcone *et al.*, Phys. Rev. Lett. **93**, 197401 (2004).
[8] J. B. Pendry, A. J. Holden, W. J. Stewart, and I. Youngs, Phys. Rev. Lett. **76**, 4773 (1996).
[9] P. A. Belov *et al.*, Phys. Rev. B **67**, 113103 (2003).
[10] B. J. Justice, J. J. Mock, L. Guo, A. Degiron, D. Schurig, and D. R. Smith, Opt. Express **14**, 8694 (2006).
[11] D. M. Pozar, *Microwave Engineering* (Wiley, New York, 1998), 2nd ed.
[12] R. E. Collin, *Field Theory of Guided Waves* (IEEE Press, New York, 1990), 2nd ed., Problem 8.2.
[13] D. R. Smith, S. Schultz, P. Markos, and C. M. Soukoulis, Phys. Rev. B **65**, 195104 (2002).
[14] R. B. Greegor, C. G. Parazzoli, J. A. Nielsen, M. A. Thompson, M. H. Tanielian, and D. R. Smith, Appl. Phys. Lett. **87**, 091114 (2005).
[15] T. Driscoll, D. N. Basov, A. F. Starr, P. M. Rye, S. Nemat-Nasser, D. Schurig, and D. R. Smith, Appl. Phys. Lett. **88**, 081101 (2006).
[16] D. R. Smith and J. B. Pendry, J. Opt. Soc. Am. B **23**, 391 (2006).
[17] A. P. Hibbins, M. J. Lockyear, and J. R. Sambles, J. Appl. Phys. **99**, 124903 (2006).